Available online at www.sciencedirect.com

ScienceDirect

Proceedings of the Combustion Institute 35 (2015) 589–596

Proceedings of the Combustion Institute

www.elsevier.com/locate/proci

Optimization of a hydrogen combustion mechanism using both direct and indirect measurements

T. Varga [a,b], T. Nagy [a,c], C. Olm [a,b], I.Gy. Zsély [a], R. Pálvölgyi [a], É. Valkó [a,b], G. Vincze [a], M. Cserháti [a], H.J. Curran [d], T. Turányi [a,*]

[a] Institute of Chemistry, Eötvös University (ELTE), Budapest, Hungary
[b] MTA-ELTE Research Group on Complex Chemical Systems, Budapest, Hungary
[c] Institute of Materials and Environmental Chemistry, MTA Research Centre for Natural Sciences, Budapest, Hungary
[d] Combustion Chemistry Centre, National University of Ireland, Galway (NUIG), Ireland

Available online 5 July 2014

Abstract

The Kéromnès et al. (2013) mechanism for hydrogen combustion has been optimized using a large set of indirect experimental data, consisting of ignition measurements in shock tubes (566 datapoints in 43 datasets) and rapid compression machines (219/19), and flame velocity measurements (364/59), covering wide ranges of temperature (800 K–2300 K), pressure (0.1 bar–65 bar) and equivalence ratio ($\varphi = 0.2$–5.0). According to the sensitivity analysis carried out at each experimental datapoint, 30 Arrhenius parameters and 3 third body collision efficiency parameters of 11 elementary reactions could be optimized using these experimental data. 1749 directly measured rate coefficient values in 56 datasets belonging to the 11 reaction steps were also utilized. Prior uncertainty ranges of the rate coefficients were determined from literature data. Mechanism optimization has led to a new hydrogen combustion mechanism, a set of newly recommended rate parameters with their covariance matrix, and temperature-dependent posterior uncertainty ranges of the rate coefficients. The optimized mechanism generated here was tested together with 13 recent hydrogen combustion mechanisms and proved to be the best one.

Keywords: Hydrogen combustion; Detailed mechanisms; Mechanism optimization; Parameter uncertainty

1. Introduction

The reaction mechanism of hydrogen combustion plays a central role in combustion chemistry. Several new hydrogen combustion mechanisms were published in the last years; see e.g., the reviews of Ó Conaire et al. [1], Konnov [2], Hong et al. [3], Burke et al. [4], and Kéromnès et al. [5]. In all of these mechanisms, most of the parameters were based on directly measured or theoretically calculated rate coefficients, but also some of the rate parameters were tuned to improve the agreement with measured ignition delay times or flame velocities. These types of experimental

* Corresponding author. Address: Institute of Chemistry, Eötvös University (ELTE), P.O. Box 32, 1518 Budapest, Hungary. Fax: +36 1 372 2592.
E-mail address: turanyi@chem.elte.hu (T. Turányi).

http://dx.doi.org/10.1016/j.proci.2014.06.071
1540-7489/

data are usually referred to as indirect measurements, since such experimental results can be compared with simulation results based on a detailed mechanism. Although these mechanisms contain almost identical reaction steps and were developed by utilizing a similar set of experiments, several of the rate parameters and also the performance of the mechanisms at various experimental conditions are different [6].

Mechanism optimization is the process during which the rate parameters of several reaction steps are systematically changed within their uncertainty limits to achieve a better reproduction of experimental results. The first articles in this topic were written by Frenklach and Miller [7–9] and an algorithm was described in the article of Frenklach, Wang, and Rabinowitz [10]. The most widely used optimized mechanism is the GRI-Mech 3.0 [11]. Frenklach et al. extended the mechanism optimization approach towards data collaboration [12–16], recommending the services of the PrIMe website [17] and the application of the PrIMe data format [15]. Another series of mechanism optimization papers was published by Wang et al., who applied this approach to the combustion mechanisms of syngas [18], ethylene [19], propane [20], and *n*-heptane [21].

In the mechanism optimization works of Frenklach et al. and Wang et al. "optimization targets", based on indirect measurement data, were selected and the most influential rate parameters (called "active parameters") were identified by local sensitivity analysis. They optimized *A*-factors of the rate expressions, third body collision efficiency parameters, and enthalpies of formation. During the parameter optimization, the simulation results were calculated indirectly, using polynomial surrogate models ("response surfaces"). Both Frenklach et al. and Wang et al. reported that a large number of the obtained optimized *A*-factors were at the edges of their uncertainty interval, which usually meant a factor of 2 or 3 difference from the previously recommended values. To overcome this problem, in their recent works [16,21–23] the objective function was extended in such a way that deviation from the evaluated *A*-factor (determined on the basis of direct measurements) was penalized, and therefore the *A*-factors optimized in this way were closer to the evaluated ones.

Cai and Pitsch [24] suggested optimization of rate rules for larger hydrocarbon models, which reduce the dimensionality of the task and also guarantee the consistency of rate coefficients of kinetically similar reactions. This approach is not applicable for the combustion mechanisms of small fuel molecules.

Davis et al. [18] produced an optimized syngas combustion mechanism, including a hydrogen combustion mechanism subset. They considered 36 (22) optimization targets, including 12 (6) measured laminar flame velocities, 2 (2) concentration maxima in flat flames, 10 (6) flow reactor measurements and 12 (8) ignition delay measurements in shock tubes. The original mechanism consisted of 14 (11) species and 30 (20) reactions. Optimization of 28 (21) rate parameters (including 22 (16) *A*-factors and 6 (5) 3rd body efficiencies) was then carried out. The numbers in parentheses refer to the values belonging to the hydrogen subsystem. The optimized mechanism of Davis et al. [18] became highly successful and was used in many modeling studies.

You et al. [23] recently published an article about the PrIMe Workflow Application. The applicability of this software was demonstrated by the optimization of a hydrogen combustion mechanism, considering 8 ignition delay times measured in shock tubes and 4 flow reactor measurements. The authors optimized the *A*-factors of all of the 21 reaction steps. The obtained mechanism is applicable within the PrIMe modeling framework and the authors did not publish it in CHEMKIN format.

The methodology used here has several similarities and differences compared to the methods used by the authors above. We also apply local sensitivity analysis for the identification of active parameters, the PrIMe data format [17], and response surfaces for improving the numerical efficiency. The differences are that (i) we use a large number of indirect experimental data (instead of selected optimization targets), (ii) all Arrhenius parameters are optimized (instead of only the *A*-factors) and (iii) new approaches are used for the generation of response surfaces and global parameter estimation. Agreement of the optimized parameters with the previous rate parameter evaluations is achieved by taking into account direct measurements of rate coefficients on which the evaluations had been based, instead of guiding the optimized parameters towards the evaluated values. The methodology applied here has been described in detail in a previous article [25].

The hydrogen combustion mechanism of Kéromnès et al. [5] was selected as the initial mechanism on the basis of our previous investigations [6], since this mechanism provided the best overall description of the experimental data. The optimization is based on 1149 indirect measurements (ignition delay times measured in shock tubes and rapid compression machines (RCMs), and flame velocities), and also on 1749 direct measurements of the rate coefficients of important reaction steps. 33 rate parameters were optimized here, including 30 Arrhenius parameters and 3 third body collision efficiency parameters of 11 elementary reactions. The optimized mechanism obtained was tested together with 13 recently published hydrogen combustion mechanisms.

2. Collection of indirect experimental data

A large set of indirect experimental data was collected for hydrogen combustion, consisting of ignition delays in shock tubes (786 datapoints in 54 datasets from 16 publications) and RCMs (229 datapoints in 20 datasets from three publications), flame velocity measurements (631 datapoints in 73 datasets from 22 publications), concentration–time profiles in jet-stirred reactors (JSRs) (149 datapoints in 9 datasets from one publication) and concentration–time profiles in flow reactors (372 datapoints in 16 datasets from two publications). Burke et al. [4] found that simulated speciated flame measurement data are not sensitive to the kinetic parameters. Our calculations have also confirmed this observation, therefore such data were not used here.

A dataset contains those datapoints that were consecutively measured using the same apparatus at similar conditions except for one condition that was systematically varied. These data include all measurements that had been used in the mechanism development works of Ó Conaire et al. [1], Konnov [2], Hong et al. [3], Burke et al. [4], and Kéromnès et al. [5], but our collection is much wider and also includes many additional experimental data. A detailed list of the collected data can be found in Tables S1–S5 of the Supplemental Material. All experimental data were encoded in PrIMe file format [17], which is an XML scheme for the systematic storage of combustion experiments.

A MATLAB code called Optima was used for simulating the combustion experiments, local sensitivity analysis, response surface generation, mechanism optimization, and testing reaction mechanisms against the experimental data. The code reads the PrIMe data files, prepares the corresponding CHEMKIN-II [26] input file, starts the appropriate simulation program (SENKIN [27], PREMIX [28] or PSR [29]) of the CHEMKIN-II package, and processes the simulation results.

The collected set of experimental data has been used in a recent paper [6] to test the performance of 19 recently published hydrogen combustion mechanisms (including the hydrogen combustion part of syngas and selected hydrocarbon combustion mechanisms). These calculations indicated that ignition delay times measured in shock tubes at temperatures below 1000 K were poorly reproduced by all mechanisms. At these conditions the pressure behind the reflected shock wave cannot be considered constant in time [30], and in the early shock tube measurements the pressure–time profiles were not reported which could be used to take into account this effect. These low-temperature shock tube data (131 datapoints) were excluded from both the optimization and mechanism testing. All RCM measurements were accompanied with measured pressure profiles; therefore the low-temperature RCM data could be used. Flow reactor experiments were interpreted by the authors by shifting the simulated species profiles to match the simulated half fuel depletion time with the experiments [31,32]. We used the same type of time shifting in all our simulations. However, this introduces a free parameter during optimization and allows for an underestimation of systematic differences between the model and experimental results. For this reason these experiments were not included in our optimization, but still used for the mechanism comparisons. Also, only experimental results between fuel depletion of 90% and 10% were taken into account. The rate parameters showed relatively low sensitivity at the conditions of the JSR datapoints and therefore these points were not considered in the optimization, but were used for mechanism testing.

3. Selection of rate parameters to be optimized

Local sensitivity analysis at the conditions of the indirect experimental data was carried out based on the Kéromnès mechanism. For each simulated experimental datapoint, the sensitivities of the simulation result with respect to the A-factors of each reaction step and (if applicable) to the third body efficiencies were calculated. We selected the rate parameters of those reactions for optimization that produced high sensitivity coefficient values at several experimental conditions. The list of the rate parameters chosen for optimization is given in Table 1. Altogether, 30 Arrhenius parameters of 11 reactions and the third body collision efficiencies of Ar, H_2 and H_2O of reaction R9 $H + O_2 + M = HO_2 + M$ were selected. For reactions R8, R9 and R16, the Arrhenius parameters refer to the low-pressure limit. The third body collision efficiencies of reactions R8 and R16 did not show a high importance, nor did the other collision efficiency parameters of reaction R9. For most selected reactions all three Arrhenius parameters (A, n, E) were optimized. In the case of reactions R9, R11 and R15, two Arrhenius parameters were sufficient to describe the temperature dependence of the rate coefficient, therefore only two parameters were optimized for these reactions.

4. Determination of the *a priori* uncertainty domain of the parameters

Global parameter optimization methods require a definition of the domain of uncertainty of the parameters, because the optimal parameter set is sought within this domain. Also, the aim of the present optimization was to find physically realistic rate parameters and therefore the *a priori*

Table 1
Reactions selected for optimization, the number of direct measurements used for optimization and the optimized values of the parameters. For reactions with a third body (+M) the optimized parameters refer to the low-pressure limit.

Optimized subset of reactions		Number of direct measurements		Optimized parameters (units: mol, cm^3, s, K)		
		Datapoints	Datasets	ln A	n	E/R
R1	$H + O_2 = O + OH$	745	9	30.25	0.2434	7265
R2	$O + H_2 = H + OH$	338	11	10.21	2.750	3208
R3	$OH + H_2 = H + H_2O$	181	7	16.90	1.803	1612
R8	$H + OH + M = H_2O + M$	6	3	55.54	−2.600	−56.84
R9 [a,b]	$H + O_2 + M = HO_2 + M$	194	10	44.38	−1.239	–
R10	$HO_2 + H = H_2 + O_2$	28	1	23.16	1.083	278.7
R11	$HO_2 + H = OH + OH$	–	–	31.79	–	119.3
R13	$HO_2 + OH = H_2O + O_2$	67	4	19.49	1.441	−1080
R15	$HO_2 + HO_2 = H_2O_2 + O_2$	73	4	32.45	–	5253
R16	$OH + OH + M = H_2O_2 + M$	113	6	35.21	−0.2033	−2175
R18	$H_2O_2 + H = H_2 + HO_2$	4	1	40.32	−1.249	3738

[a] Consisting of 40 datapoints in 4 datasets measured in N_2 bat h gas and 154 datapoints in 6 datasets measured in Ar bath gas.
[b] Optimized values of 3rd body collision efficiency parameters ($\pm 1\sigma$) of reaction $H + O_2 + M = HO_2 + M$: $m(H_2) = 1.48 \pm 1.0$, $m(Ar) = 0.540 \pm 0.011$, $m(H_2O) = 12.03 \pm 0.53$.

uncertainty domain of rate parameters had to be determined from direct measurements and from theoretical calculations found in the literature. Articles that report the results of direct measurements provide the values of the measured rate coefficient of an elementary reaction at various temperatures, pressures and possibly using different bath gases.

The method for determining the prior uncertainty domain of the Arrhenius parameters has previously been described in detail [25] for two elementary reactions and a similar treatment was used here for all 11 reaction steps. For each elementary reaction investigated, all direct measurements and theoretical determinations of the rate coefficient were collected from the NIST Chemical Kinetics Database [33] and from review articles [1–5]. On an Arrhenius plot, the temperature dependence of ln k outlines an uncertainty band of the rate coefficient. The distance of the k^{min} and k^{max} limits from the centerline defines the $f(T)$ temperature-dependent uncertainty parameter. The $f(T)$ points were converted to the prior covariance matrix of the Arrhenius parameters [34,35]. Also, the width of the uncertainty band was used as the limiting value of the acceptable rate coefficients during the optimization. For reactions R15 and R18, very little literature information was available and constant $f = 0.4$ and $f = 0.6$ were estimated, respectively. The $f(T)$ functions obtained can be seen in Fig. S1 of the Supplemental Material. Little information was available on the uncertainty of the third body efficiency parameters of reaction R9. In the optimization, we used non-restrictive uncertainty ranges $m(H_2) = 1.30 \pm 1.25$, $m(Ar) = 0.5 \pm 0.4$ and $m(H_2O) = 10 \pm 6$.

5. Collection of relevant direct measurement data

The next step was the collection of reliable direct measurement data for the selected reaction steps. Not all direct measurements used at the determination of the uncertainty limits were utilized, but only 1749 datapoints in 56 datasets from 42 publications that were considered reliable by the review articles. The number of direct measurements used for each reaction step is given in Table 1 and the detailed list can be seen in Table S6 of the Supplemental Material. All direct measurement results (i.e., rate coefficient values) together with the conditions of determinations were also encoded in PrIMe file format [17].

6. Calculation of response surfaces

A polynomial response surface was calculated for each indirect measurement. The active parameters (Arrhenius-parameters and third body collision efficiencies), previously identified by sensitivity analysis, were uniformly sampled within the uncertainty range defined by the corresponding *a priori* $f(T)$ functions. 10,000 samples of the active parameters were generated for each datapoint, all other parameters were fixed at their original values, and the experiment was simulated using each parameter set. The simulation results were fitted by orthonormal polynomials using the method described in [36]. To generate a fast surrogate model, monomials were restricted to be at most 4th order and to have up to two variables of which one is first order. The orthonormal polynomial expansions were then converted to regular polynomials [36].

The polynomials obtained were tested against simulation results generated from 500 new, random sets of parameters. The maximum allowed difference between the test set of simulation results and the polynomial was the 1σ experimental uncertainty of the measurement. Using this criterion, a satisfactory response surface was obtained for most of the datapoints. For ignition delay times and flame velocities, average error of the response surface was about 0.5% and 0.05 cm/s, respectively. Accurate response surfaces could be created for about 80% of the indirect experimental data, including 538 ignition delay measurements in shock tubes from 54 datasets, 153 ignition delay measurements in RCMs from 20 datasets and 475 flame velocity measurements from 70 datasets. In the case of three datasets (×2000010, ×20000011 and ×20000054 in Table S3), accurate response surfaces could not be generated for any of the datapoints. These datasets were not used for optimization, but included in the final comparison.

Table 2
Error function values calculated for the initial and the optimized mechanisms.

Measurement type	Kéromnès mechanism	Optimized mechanism
Shock tube	1.081	1.043
RCM	1.400	0.600
Flame velocities	3.115	1.770
Direct measurements	2.254	0.924
Total	7.851	4.338

7. Parameter optimization

The global parameter optimization method applied here has been described in detail in [25] and it has also been used in [37] and [38]. The optimal set of parameters was achieved by the minimization of the following objective function:

$$E(p) = \frac{1}{N}\sum_{i=1}^{N}\frac{1}{N_i}\sum_{j=1}^{N_i}\left(\frac{Y_{ij}^{\mathrm{mod}}(p) - Y_{ij}^{\mathrm{exp}}}{\sigma\left(Y_{ij}^{\mathrm{exp}}\right)}\right)^2 \quad (1)$$

Here N is the number of datasets and N_i is the number of datapoints in the i-th dataset. Values y_{ij}^{exp} and $\sigma(y_{ij}^{\mathrm{exp}})$ are the j-th measured datapoint and its standard deviation, respectively, in the i-th dataset. The experimental standard deviation was determined for each dataset separately, based on their scatter. The estimated standard deviations are listed in Tables S1–S6 of the Supplemental Material. Constant absolute error ($\sigma(y_{ij}^{\mathrm{exp}})$ identical for all j) was assumed for the measured flame velocities, in this case $Y_{ij} = y_{ij}$. Constant relative error ($\sigma(\ln y_{ij}^{\mathrm{exp}})$ identical for all j and $Y_{ij} = \ln y_{ij}$) was assumed for the ignition delay measurements and the rate coefficients determined in direct experiments. For the indirect measurement data, the simulated (modeled) value is Y_{ij}^{mod}, which is obtained from a simulation using an appropriate detailed mechanism. For the direct measurements, the corresponding modeled value Y_{ij}^{mod} is calculated using the appropriate expression of the rate coefficient at a given temperature, pressure, and bath gas composition.

The optimization involved the fitting of 33 parameters to approximately 3000 datapoints which is a computationally challenging task, therefore a

Table 3
Comparison of error function values between our optimized and 13 recently published mechanisms by experiment type. The error function values are normalized by the number of datasets within each column.

Mechanism	Ref.	Average error function						Total (w/o He)	Total
		Shock tube	RCM	JSR	Flow reactors	Flames	Flames (w/o He)		
Optimized mechanism	This work	5.94	6.70	2.97	8.08	4.86	6.11	**5.32**	**4.96**
Kéromnès 2013	[5]	6.69	11.33	3.02	13.25	8.11	5.88	**7.62**	**8.29**
NUIG NGM 2010	[41]	7.92	17.08	3.00	7.27	7.24	9.94	**9.53**	**8.45**
Ó Conaire 2004	[1]	8.51	23.15	2.96	8.18	–	8.90	**10.44**	–
Konnov 2008	[2]	9.67	27.61	3.06	10.91	–	6.37	**11.04**	–
Hong 2011	[3]	11.45	9.15	3.01	8.15	–	18.72	**12.40**	–
Li 2007	[39]	7.58	43.98	2.99	7.83	7.61	7.07	**12.69**	**12.04**
Burke 2012	[4]	13.29	48.54	3.06	3.91	4.57	5.91	**14.57**	**12.65**
Saxena Williams 2006	[40]	11.06	47.28	3.02	28.30	7.60	8.13	**17.05**	**15.43**
San Diego 2014	[44]	16.80	17.75	3.00	14.90	25.22	17.62	**13.86**	**17.22**
CRECK 2012	[42]	6.61	28.42	2.93	21.44	25.49	38.30	**21.32**	**18.58**
Davis 2005	[18]	11.62	93.55	3.00	4.89	5.84	7.58	**21.52**	**18.60**
GRI 3.0 1999	[11]	49.07	115.6	2.42	11.56	–	23.97	**43.78**	–
Sun 2007	[43]	11.99	309.2	3.11	25.42	15.31	18.60	**60.50**	**52.55**
No. of datapoints		566	219	149	191	432	319	**1390**	**1513**
No. of data sets		43	19	9	14	62	39	**121**	**145**

The bold values in the last two columns mark the weighted sum of the previous columns. These were the values used for the ordering of the mechanisms (rows) and we intended to emphasize these values.

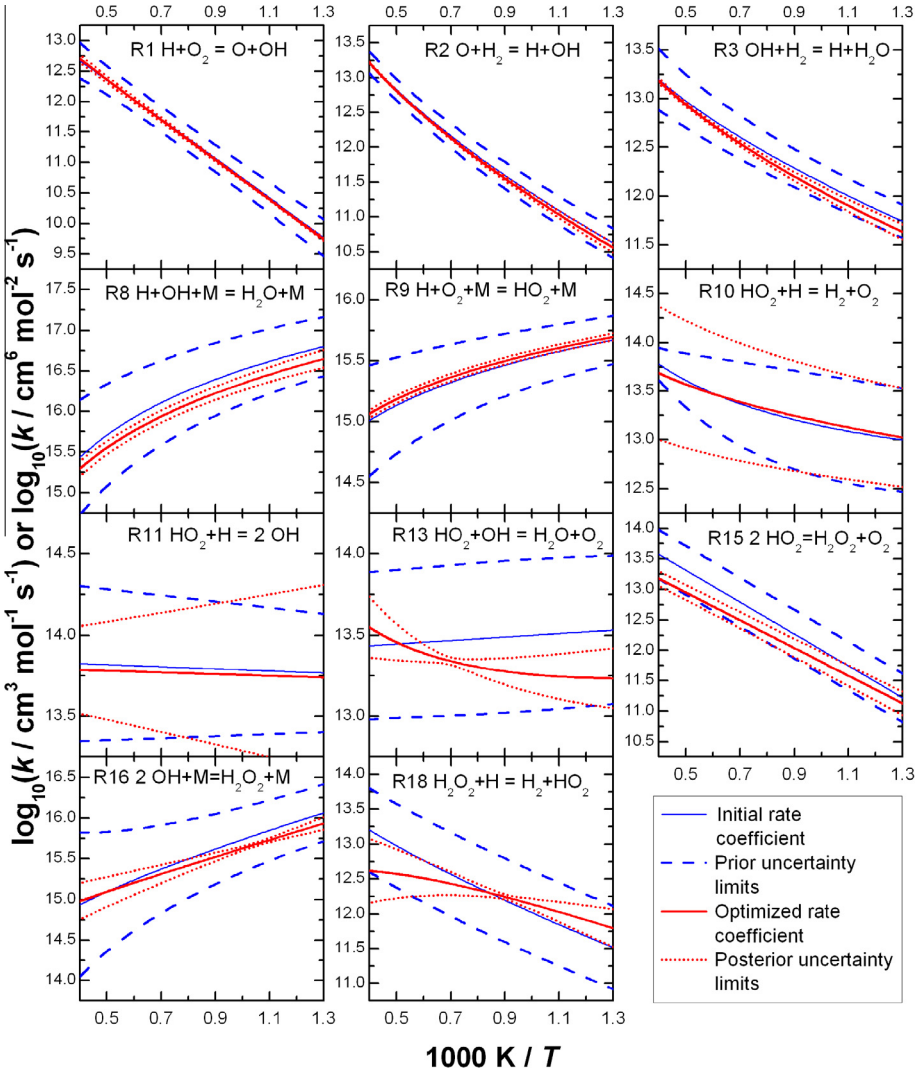

Fig. 1. Arrhenius plots of the initial and optimized rate coefficients with their prior and posterior uncertainty ranges for the 11 optimized elementary reactions. Rate coefficient units are $cm^6\ mol^{-2}\ s^{-1}$ for reactions R8, R9 and R16, and the units are $cm^3\ mol^{-1}\ s^{-1}$ for the other reactions.

systematic hierarchical optimization strategy was devised. In the first optimization step those experimental data were selected as optimization targets that were sensitive only to the parameters of the lowest number of reactions (R1 and R9). Then more and more experimental data and the corresponding influential reactions were included following the same concept and all parameters considered up to that point were optimized. This resulted in the inclusion of further reactions in the following order: R2, R3, R10, R8, R11, R13, R18, R16 and R15.

In the first stage, a complete hierarchical optimization was carried out using the response surfaces only. Starting from the newly obtained parameter set, in the second optimization stage the ignition delay times were calculated with SENKIN directly and not via the response surfaces, while the computationally more expensive laminar flame calculations were still performed with the surrogate models. This allowed for the elimination of the error caused by the potential inaccuracies of the response surfaces of the ignition experiments. Also, in this way ignition experiments for which accurate response surfaces could not be generated were also taken into account. However, the difference between the optimized parameter sets obtained in the first and second stages of optimization was not significant. Afterwards all experimental datasets that could not be reproduced within 4σ of the experimental uncertainty by the model obtained in the previous step were excluded from

the final optimization step. Eleven shock tube, one RCM and eleven flame data sets were excluded this way, and are marked in Tables S1–S3.

In the final optimization cycle, 566 datapoints of shock tube and 219 datapoints of RCM ignition measurements were used, together with 364 flame velocity measurements and 1749 direct measurements. Table 1 presents the optimized values of the rate parameters. The complete optimized mechanism is given in the Supplemental Material in CHEMKIN format together with the transport data file. Table 2 shows that the value of the objective function (1) decreased significantly as a result of the optimization, and also the description of the experimental data improved in each data category separately.

8. Investigation of the optimized mechanism

The performance of the optimized mechanism was compared to 13 hydrogen combustion mechanisms that were mainly published in the last decade. The mechanisms used for comparisons included the hydrogen combustion mechanisms of Ó Conaire et al. [1], Konnov [2], Hong et al. [3] and Burke et al. [4] and other mechanisms [5,18,39–44] that were originally developed for syngas, hydrocarbon or oxygenate combustion, but were also validated for hydrogen combustion data. The simulations were carried out with the CHEMKIN codes and response surfaces were not used here. The flame, JSR and flow reactor experiments not considered in the optimization were also taken into account. The datasets that were excluded from the final optimization (marked in Tables S1–S3) were also considered in this comparison.

The calculated error function values are given in Table 3. In each column, these values are normalized by the number of datasets. The total error function values are the dataset weighted sums of the values belonging to each category. Some mechanisms [1–3,11] do not contain He as a bath gas, and according to our simulations cannot reproduce well the experiments with He. Therefore, flame velocity experiments with and without helium diluent are indicated separately in Table 3. This table shows that the optimized mechanism gives the best overall reproduction of all available experimental data, although it is not the best in each category, since Burke-2012 [4] is better at reproducing the flame velocity and flow reactor measurements, while GRI-Mech 3.0 [11] is better at reproducing the JSR outlet concentrations.

9. The *a posteriori* uncertainty of the determined parameters

The covariance matrix of all fitted parameters was calculated using the equation published in [25]. This covariance matrix characterizes the joint *a posteriori* domain of uncertainty of the parameters and it can be transformed to the $f(T)$ posterior uncertainty function of each investigated reaction step [25]. The optimized rate coefficient functions never reached their prior uncertainty limits in the investigated temperature range of 800 K to 2300 K. Figure 1 shows the temperature dependence of the original and the optimized rate coefficients for each reaction step, and the prior and posterior uncertainty bands. The mechanism optimization process resulted in a narrower and better established uncertainty band of the rate parameters for most of the reactions investigated. Figure 1 shows that the initial and optimized rate coefficients are significantly different for reactions R13, R15 and R18. These are all HO_2 radical reactions and, according to the sensitivity analysis results, these rate coefficients were mainly constrained by lean flame velocity measurements.

10. Conclusions

An optimization of the hydrogen combustion mechanism of Kéromnès et al. [5] is presented in this article. A large amount of experimental data was collected from the literature including ignition delay time, flame velocity, and JSR measurements. The local sensitivity coefficients of the simulated experimental datapoints were determined, and the results indicated that rate parameters of 11 reactions (in total 30 Arrhenius parameters and 3 third body collision efficiency parameters) have a high influence on the simulation results. All direct measurements and theoretical determinations belonging to these 11 elementary reactions were collected and used to outline the *a priori* uncertainty band of the rate coefficients. The optimization took into account both direct and indirect measurements, and yielded optimized values of these parameters. It also provided posterior uncertainty bands for the rate coefficients, which were usually narrower than the prior ones. The performance of the optimized mechanism was compared with those of several recently published mechanisms and it is demonstrated that our optimized hydrogen combustion mechanism provides the best overall description of the currently available ignition delay time, laminar flame velocity, JSR exit concentration and flow reactor measurements, while all rate coefficients are consistent with the respective direct measurements.

Acknowledgements

The authors acknowledge the helpful discussions with Prof. M. J. Pilling, and the financial support of OTKA grants K84054 and NN100523.

The authors are also grateful for the comments of the partners in COST collaboration CM0901 Detailed Chemical Models for Cleaner Combustion.

Appendix A. Supplementary data

Supplementary data associated with this article can be found, in the online version, at http://dx.doi.org/10.1016/j.proci.2014.06.071.

References

[1] M. Ó Conaire, H.J. Curran, J.M. Simmie, W.J. Pitz, C.K. Westbrook, *Int. J. Chem. Kinet.* 36 (2004) 603–622.
[2] A.A. Konnov, *Combust. Flame* 152 (2008) 507–528.
[3] Z. Hong, D. Davidson, R. Hanson, *Combust. Flame* 158 (2011) 633–644.
[4] M. Burke, M. Chaos, Y. Ju, F.L. Dryer, S. Klippenstein, *Int. J. Chem. Kinet.* 44 (2012) 444–474.
[5] A. Kéromnès, W.K. Metcalfe, K.A. Heufer, N. Donohoe, A.K. Das, C.-J. Sung, J. Herzler, C. Naumann, P. Griebel, O. Mathieu, M.C. Krejci, E.L. Petersen, W.J. Pitz, H.J. Curran, *Combust. Flame* 160 (2013) 995–1011.
[6] C. Olm, I.G. Zsély, R. Pálvölgyi, T. Varga, T. Nagy, H.J. Curran, T. Turányi, Combust. Flame (2013) in press, available on line, http://dx.doi.org/10.1016/j.combustflame.2014.1003.1006.
[7] D. Miller, M. Frenklach, *Int. J. Chem. Kinet.* 15 (1983) 677–696.
[8] M. Frenklach, *Combust. Flame* 58 (1984) 69–72.
[9] M. Frenklach, D.L. Miller, *AIChE J.* 31 (1985) 498–500.
[10] M. Frenklach, H. Wang, M.J. Rabinowitz, *Prog. Energy Combust. Sci.* 18 (1992) 47–73.
[11] G.P. Smith, D.M. Golden, M. Frenklach, N.W. Moriary, B. Eiteneer, M. Goldenberg, C.T. Bowman, R.K. Hanson, S. Song, W.C. Gardiner, V.V. Lissianski, Z. Qin: GRI-Mech 3.0, available at http://www.me.berkeley.edu/gri_mech/.
[12] R. Feeley, P. Seiler, A. Packard, M. Frenklach, *J. Phys. Chem. A* 108 (2004) 9573–9583.
[13] M. Frenklach, A. Packard, P. Seiler, R. Feeley, *Int. J. Chem. Kinet.* 36 (2004) 57–66.
[14] R. Feeley, M. Frenklach, M. Onsum, T. Russi, A. Arkin, A. Packard, *J. Phys. Chem. A* 110 (2006) 6803–6813.
[15] M. Frenklach, *Proc. Combust. Inst.* 31 (2007) 125–140.
[16] X.Q. You, T. Russi, A. Packard, M. Frenklach, *Proc. Combust. Inst.* 33 (2011) 509–516.
[17] M. Frenklach: PrIMe Webpage, available at http://www.primekinetics.org/.
[18] S. Davis, A. Joshi, H. Wang, F. Egolfopoulos, *Proc. Combust. Inst.* 30 (2005) 1283–1292.
[19] D.A. Sheen, X. You, H. Wang, T. Lovas, *Proc. Combust. Inst.* 32 (2009) 535–542.
[20] W.J. Qin, V.V. Lissianski, H. Yang, W.C. Gardiner, S.G. Davis, H. Wang, *Proc. Combust. Inst.* 28 (2000) 1663–1669.
[21] D.A. Sheen, H. Wang, *Combust. Flame* 158 (2011) 645–656.
[22] D.A. Sheen, H. Wang, *Combust. Flame* 158 (2011) 2358–2374.
[23] X.Q. You, A. Packard, M. Frenklach, *Int. J. Chem. Kinet.* 44 (2012) 101–116.
[24] L.M. Cai, H. Pitsch, *Combust. Flame* 161 (2014) 405–415.
[25] T. Turányi, T. Nagy, I.G. Zsély, M. Cserháti, T. Varga, B.T. Szabó, I. Sedyó, P.T. Kiss, A. Zempléni, H.J. Curran, *Int. J. Chem. Kinet.* 44 (2012) 284–302.
[26] R.J. Kee, F.M. Rupley, J.A. Miller, *Sandia National Laboratories*, report SAND89-8009B, 1989.
[27] A.E. Lutz, R.J. Kee, J.A. Miller, Sandia National Laboratories, report SAND87-8248, 1988.
[28] R.J. Kee, J.F. Grcar, M.D. Smooke, J.A. Miller, Sandia National Laboratories, report SAND85-8240, 1985.
[29] P. Glarborg, R.J. Kee, J.F. Grcar, J.A. Miller, Sandia National Laboratories, report SAND86-8209, 1986.
[30] G.A. Pang, D.F. Davidson, R.K. Hanson, *Proc. Combust. Inst.* 32 (2009) 181–188.
[31] R.A. Yetter, F.L. Dryer, H. Rabitz, *Combust. Sci. Technol.* 79 (1991) 129–140.
[32] M.A. Mueller, T.J. Kim, R.A. Yetter, F.L. Dryer, *Int. J. Chem. Kinet.* 31 (1999) 113–125.
[33] J.A. Manion, R.E. Huie, R.D. Levin, J.D.R. Burgess, V.L. Orkin, W. Tsang, W.S. McGivern, J.W. Hudgens, V.D. Knyazev, D.B. Atkinson, E. Chai, A.M. Tereza, C.-Y. Lin, T.C. Allison, W.G. Mallard, F. Westlet, J.T. Herron, R.F. Hampson, D.H. Frizzell: NIST Chemical Kinetics Database, NIST Standard Reference Database 17, Version 7.0 (Web Version), Release 1.4.3, Data version 2008.12, National Institute of Standards and Technology, Gaithersburg, Maryland, 20899-8320., available at http://kinetics.nist.gov.
[34] T. Nagy, T. Turányi, *Int. J. Chem. Kinet.* 43 (2011) 359–378.
[35] T. Nagy, T. Turányi, *Reliab. Eng. Syst. Safety* 107 (2012) 29–34.
[36] T. Turányi, *Comput. Chem.* 18 (1994) 45–54.
[37] I.G. Zsély, T. Varga, T. Nagy, M. Cserháti, T. Turányi, S. Peukert, M. Braun-Unkhoff, C. Naumann, U. Riedel, *Energy* 43 (2012) 85–93.
[38] T. Varga, I.G. Zsély, T. Turányi, T. Bentz, M. Olzmann, *Int. J. Chem. Kinet.* 46 (2014) 295–304.
[39] J. Li, Z. Zhao, A. Kazakov, M. Chaos, F.L. Dryer, J.J.J. Scire, *Int. J. Chem. Kinet.* 39 (2007) 109–136.
[40] P. Saxena, F.A. Williams, *Combust. Flame* 145 (2006) 316–323.
[41] D. Healy, D.M. Kalitan, C.J. Aul, E.L. Petersen, G. Bourque, H.J. Curran, *Energ. Fuel* 24 (2010) 1521–1528.
[42] CRECK modeling Group Hydrogen/CO mechanism version 1201, available at http://creckmodeling.chem.polimi.it/kinetic.html/.
[43] H. Sun, S.I. Yang, G. Jomaas, C.K. Law, *Proc. Combust. Inst.* 31 (2007) 439–446.
[44] Mechanical and Aerospace Engineering (Combustion Research), University of California at San Diego: Chemical-Kinetic Mechanisms for Combustion Applications, San Diego Mechanism, version 2014-02-17, available at http://combustion.ucsd.edu/.